

Supplementary Information

Self-Assembly of Au@Ag Core-Shell Nanocuboids into Staircase

Superstructures by Droplet Evaporation

Xianzhong Yang,^a Jing Li,^b Yuxin Zhao,^c Jianhua Yang,^d Liyan Zhou,^a Zhigao Dai,^e Xiao Guo,^a Shanjun Mu,^c Quanzhen Liu,^c Chunming Jiang,^c Mengtao Sun*,^f Jianfang Wang,^d and Wenjie Liang*^a

^aBeijing National Laboratory for Condensed Matter Physics, Institute of Physics, Chinese Academy of Sciences, Beijing, 100190, China & School of Physical Sciences, University of Chinese Academy of Sciences, Beijing, 100049, China. E-mail: wjliang@iphy.ac.cn

^bKey Laboratory of Photochemical Conversion and Optoelectronic Materials, Technical Institute of Physics and Chemistry, Chinese Academy of Sciences, Beijing, 100190, China

^cState Key Laboratory of Safety and Control for Chemicals, SINOPEC Research Institute of Safety Engineering, No. 339, Songling road, Laoshan District, Qingdao, China

^dDepartment of Physics, The Chinese University of Hong Kong, Shatin, Hong Kong SAR, China

^eLaboratory of Printable Functional Nanomaterials and Printed Electronics, School of Printing and Packaging, Wuhan University, Wuhan, 430072, China

^fBeijing Key Laboratory for Magneto-Photoelectrical Composite and Interface Science, School of Mathematics and Physics, University of Science and Technology Beijing, Beijing, 100083, China. E-mail: mengtaosun@ustb.edu.cn

Methods

Materials and Growth of the nanocuboids. Cetyltrimethylammonium bromide (CTAB, 99%) and 4-Mercaptobenzoic acid (4-MBA, 90%) were obtained from Macklin Co. Ltd. (Shanghai, China). The 300 nm SiO₂/Si wafers were purchased from SQI Co. (USA). All the chemicals were used as received without further purification. Milli-Q water (18 MΩ-cm resistivity) was used in all the experiments. Au@Ag core-shell nanocuboids were synthesized by the same methods reported before.¹⁻³ Firstly, The uncoated Au nanorods with a size of 20 nm × 70 nm (diameter × length) were synthesized using a seed-mediated growth method in aqueous solutions and were stabilized with cetyltrimethylammonium bromide (CTAB).⁴ Then the obtained Au nanorod solution was centrifuged and re-dispersed into an aqueous cetyltrimethylammonium chloride (CTAC) solution. Aqueous AgNO₃ and ascorbic acid solutions were added to produce Ag shell, forming a cuboidal shape with rectangular edges and vertices. The thickness of the shell was about 7nm. The as-prepared nanocuboids solution was centrifuged (10000 rpm, 15 min), the supernatant was discarded as much as possible, and the sedimentation was re-dispersed in different volume of deionized water with 2.5 mM CTAB. In this manner, we can adjust the NCs' concentration.

Assembly. We used the 2-stage method as reported by Xie et al.⁵ In the first stage, the 10 μL droplet was evaporated for 30min with environmental humidity of ~20% and temperature of 20 °C to create a pinned edge of the NCs. In the second stage, the sample was transferred into a homemade humidity chamber with humidity of 88±5 % and temperature of 20 °C, in which the evaporation rate is much slower so that the NCs have enough time to assemble. The whole evaporation process took about 8h. After evaporation, a ring made up of Au@Ag NCs assemblies was observed on the substrate.

Characterizations. The surface morphology for the NCs arrays were characterized by atomic force microscope (AFM, MultiMode 8, Bruker) and Hitachi S4800 SEM machine. The high resolution structure of NCs was obtained at 200 kV in a transmission electron microscope (JEOL 2010F). UV-Vis absorption spectrum of the NCs aqueous solution was measured using cuvette by a Fourier transform infrared (FTIR) spectrometers (Vertex 80V, Bruker). The contact angle was measured using Contact Angle System OCA 20 (dataphysics, Germany).

FDTD simulations. The coupling effects of Au@Ag NCs on Si/SiO₂ substrate were investigated using the finite-

difference time-domain (FDTD) method. The diameter and the length of Au nanorod core were set as 20 nm and 70 nm, respectively. The length and width of Ag shell were set as 80 nm and 34 nm with a corner radius of 4 nm. The refractive indexes of Au were referred to the data from Johnson and Christy,⁶ and that of Ag, SiO₂ and Si were from Palik.⁷

SERS studies. The silicon wafer with NCs superstructures were immersed into a 1 mM 4-MBA ethanol solution for about 3 h (if soaked too long, some NCs would desorb from the substrate), rinsed thoroughly with ethanol, and dried with nitrogen. In this process, the NCs were close packed together, and self-assembled monolayers (SAMs) were formed on the surface of NCs. All Raman spectra were carried out using a HR800 Raman spectrometer (Horiba Jobin Yvon) with 50× objective and 600 grooves/mm grating. The excitation wavelength was 785 nm with an estimated laser spot size of 1.92 μm and a laser power of 1.71 mW. The power density was about 5.9×10^8 W/m². For SERS substrate, each spectrum was recorded using an accumulation time of 5 s. For the Raman test of 4-MBA solution, 0.8M 4-MBA solution was first prepared by adding little ammonium hydroxide, then Raman spectrum was carried out with accumulation time of 150s.

Evaluation of diffusion of 4-MBA molecules into NC superstructures: The as prepared horizontal arrays were soaked into 1 mM 4-MBA ethanol solution for 45 min, then rinsed with ethanol, and dried with nitrogen. Then the SERS intensities were measured at three different layers, with layer number 4, 6, 12. Then the same sample was soaked into 4-MBA ethanol solution again for another 45 min, rinsed and measured SERS signal at same positions of different layers. Same process was repeated again for another 45min. The diffusion influence of 4-MBA molecule into our superstructure was shown in Figure S8, by plotting layer-dependent SERS enhancement effect at different soaking time.

Estimation: For 10 PM solution, each droplet (10 μL) contains 6.02×10^7 NCs, and the diameter of the coffee ring is about 4.5 mm. If the NCs are packed side by side perfectly along the circumference, there will be 45-54 NCs per NC width, namely 5-6 layers horizontal arrays. Similarly, the 50 PM solution will give 108-117 NCs per NC width, namely 12-13 layers horizontal arrays.

Figures

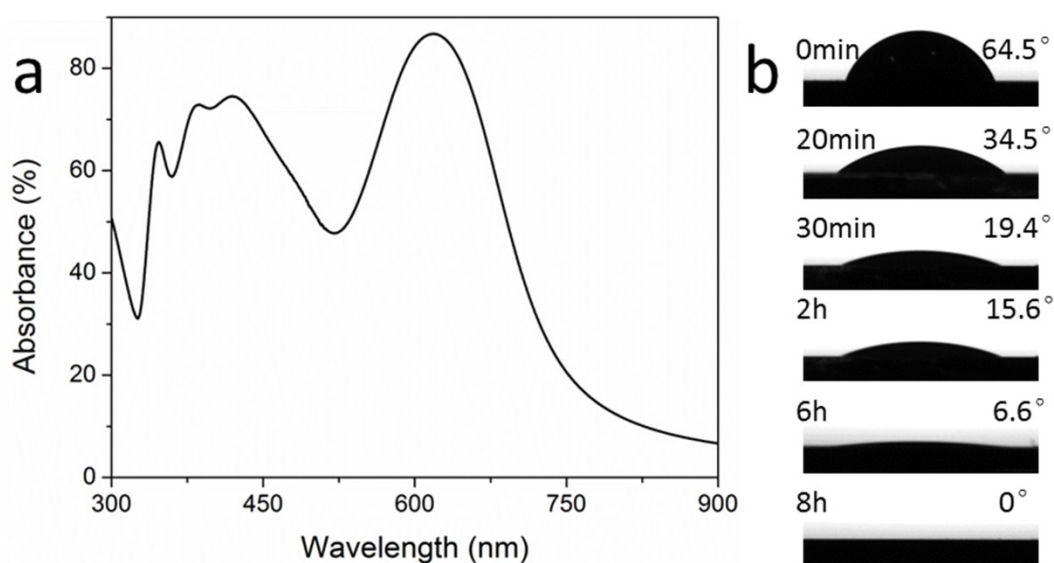


Figure S1. (a) Absorption spectrum of Au NCs aqueous solution. (b) Side views of the droplet during evaporation, the wetting angles with the change of time are labeled.

The absorption spectrum is shown in Figure S1a. The 4 plasmon peaks located at 341, 401, 465 and 630nm correspond to the dipole and multipole modes of Au@Ag core-shell nanocuboids (NCs). The wetting angles were measured and shown in Figure S1b to study the evaporation process. The contact angle was about 64.5° when the NCs solution was newly dropped onto the substrate. This state was unstable, and then the droplet relaxed to a relatively stable state quickly in several minutes with the droplet diameter reaching a maximum. Then the diameter shrunk as the solution evaporated from the edge until the pinning of the contact line. The contact angle

continuously decreased in the second stage until the solvent was completely evaporated.

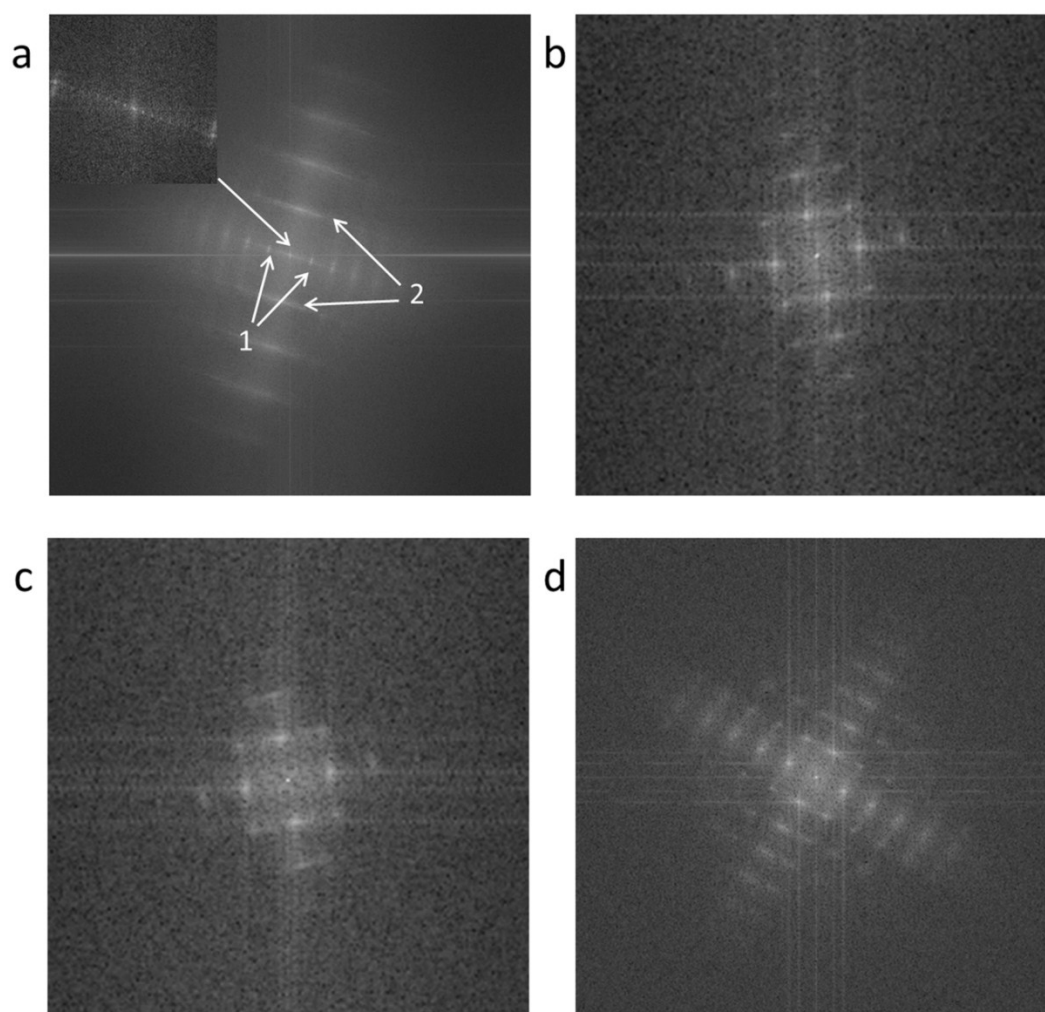


Figure S2. Fast Fourier transforms (FFT) of the ordered assemblies of different NCs nanostructures. (a) FFT of horizontal arrays shown in Figure 2a, the inset is the enlarged view of the center. FFT of vertical arrays shown in Figure 2d: (b) monolayer, (c) bilayer. (d) FFT of monolayer vertical arrays of Figure 4a.

Fast Fourier transforms (FFT) of horizontal alignment in Figure 2a is shown in **Figure S2a**. The diffuse streaks 1 result from the alignment along the longitudinal direction of NCs, with a space periodicity of 80 nm. The streaks 2 derive from the alignment along the transversal direction of NCs with a space periodicity of 34 nm. The streaks in the inset are due to the layer-by-layer horizontal stacking of NCs with a periodicity of about 720 nm. FFT of Figure S2b and S2c indicate the tetragonal packing of NCs, and they are from monolayer and bilayer vertical arrays of Figure 2d, respectively. Furthermore, streaks in these two figures have same orientation and spacing, which means the different layers of vertical arrays have same assembly orientation. Figure S2d is the FFT of monolayer vertical arrays of Figure 4a. More streaks can be recognized compared with Figure S2b, which further prove the tetragonal packing of NCs.

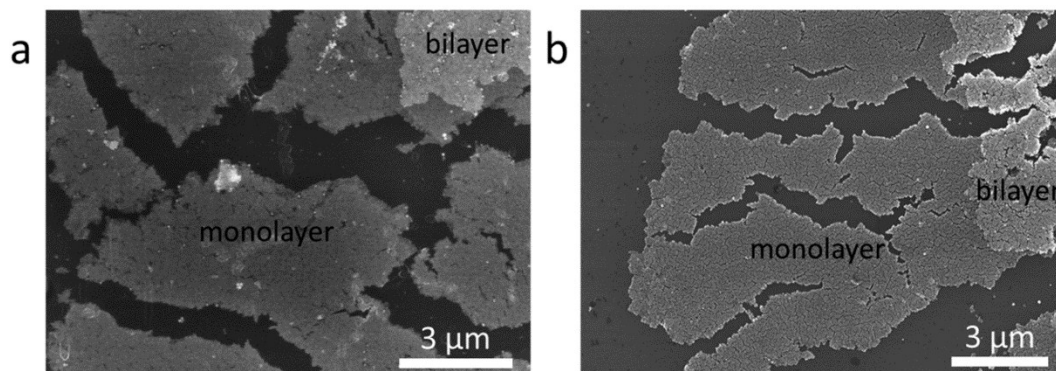


Figure S3. SEM images of vertical arrays. (a) As-fabricated vertical arrays. (b) Vertical arrays washed by ethanol.

The vertical arrays evaporated from 10 pM are shown in **Figure S3a**, they are composed of monolayer and bilayer arrays. A lot of cracks turn up after wash by ethanol (see Figure S3b).

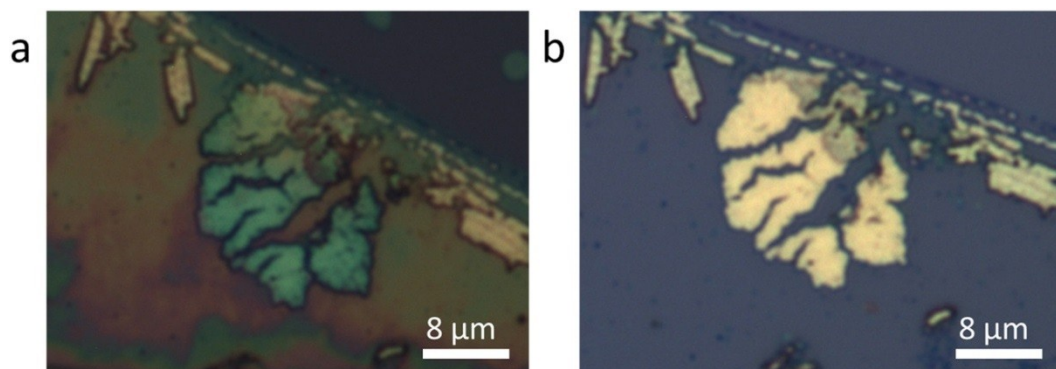


Figure S4. Optical microscopy images of vertical aligned arrays: (a) before washed by ethanol, (b) after washed by ethanol

The optical microscopy images of vertical arrays are shown in Figure S4, where we can find that the color of arrays changed from blue-green to golden yellow after the wash by ethanol.

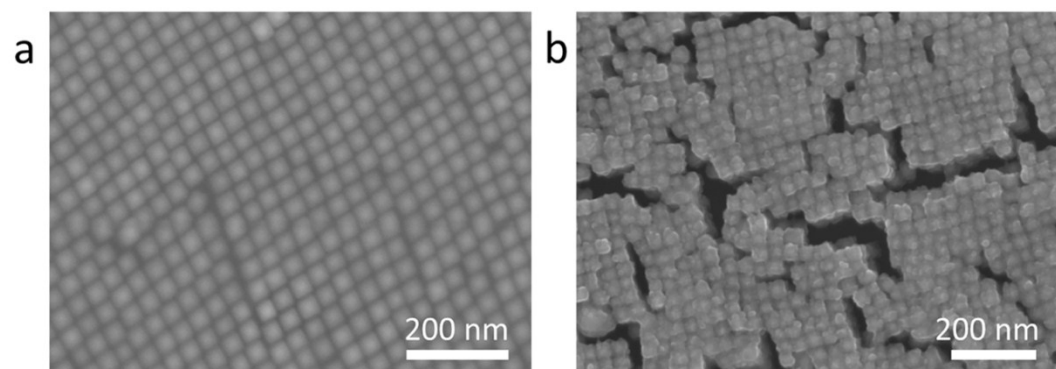


Figure S5. SEM images of vertical arrays kept in ambient air for more than one month. (a) Vertical arrays covered by CTAB layers. (b) Vertical arrays firstly washed by ethanol, and then kept in air.

Although, the coated CTAB layers make imaging difficult and plasmon enhancement effect weaker, they can protect the NCs from oxidization. The vertical assemblies coated with CTAB remain the same after being exposed in air for one month, while the NCs washed by ethanol are oxidized seriously (see **Figure S5**). Therefore, we can firstly assemble the NCs into vertical arrays, and then keep them in air. We just need to remove the CTAB before we use them.

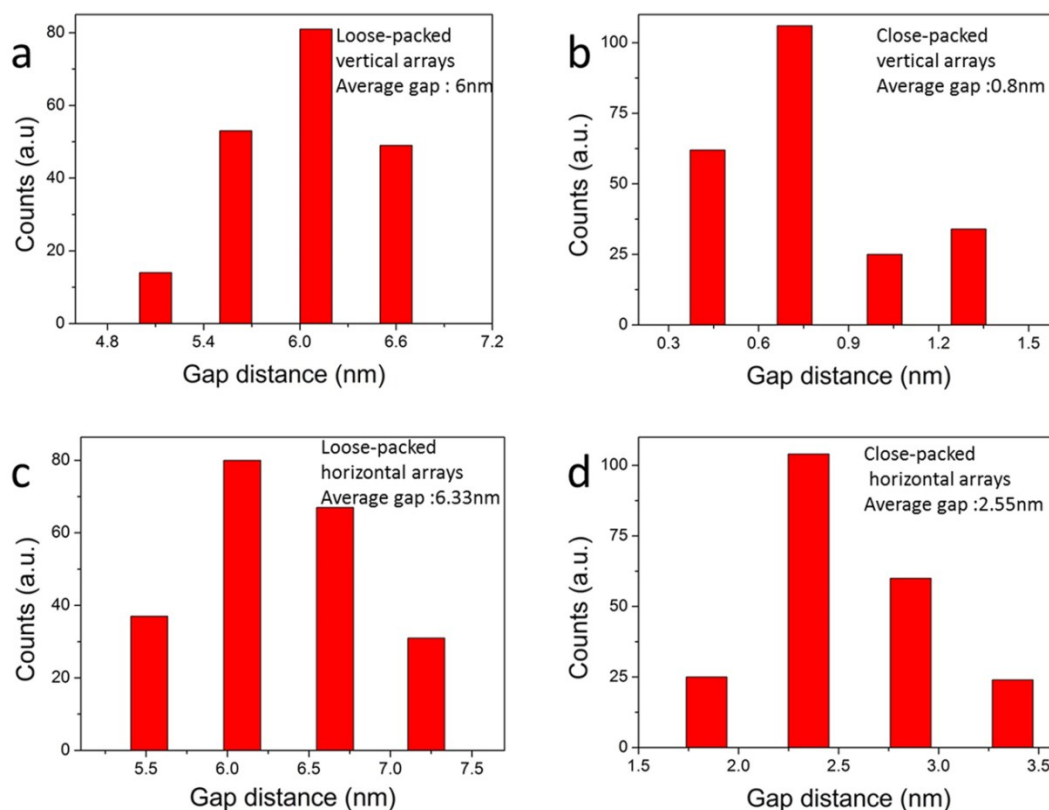


Figure S6. Gap distance distributions of different structures. (a) Loose-packed (before washed by ethanol) vertical arrays. (b) Close-packed (after washed by ethanol) vertical array. (c) Loose-packed horizontal arrays. (d) Close-packed horizontal arrays.

The gap distance can be greatly shrunk by ethanol wash, and the gap distance distributions of horizontal (along the transverse directions) and vertical arrays are shown in **Figure S6**. The average gap distances of vertical and horizontal arrays are both around 6nm before ethanol wash. Then the average gap distance of vertical arrays is reduced to 0.8nm, while that of horizontal arrays is reduced to about 2.6nm

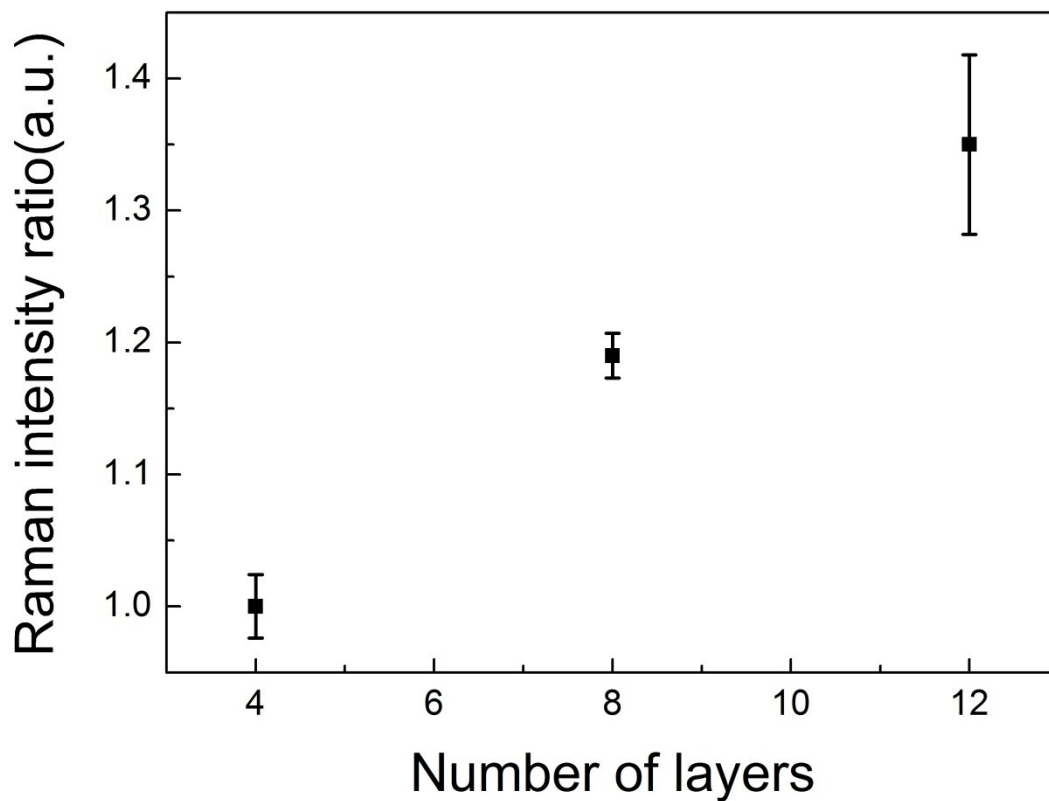


Figure S7. The Raman intensity ratio of different layers of horizontal assemblies. Raman intensity at 4 layer is taken as unit.

To check the test errors of horizontal assemblies, we carried the Raman measurement on different positions of the same layers. The results are shown in Figure S7. The test errors of 3-5, 7-9, 11-13 layers were about 2.4%, 1.7%, 6.8%, respectively.

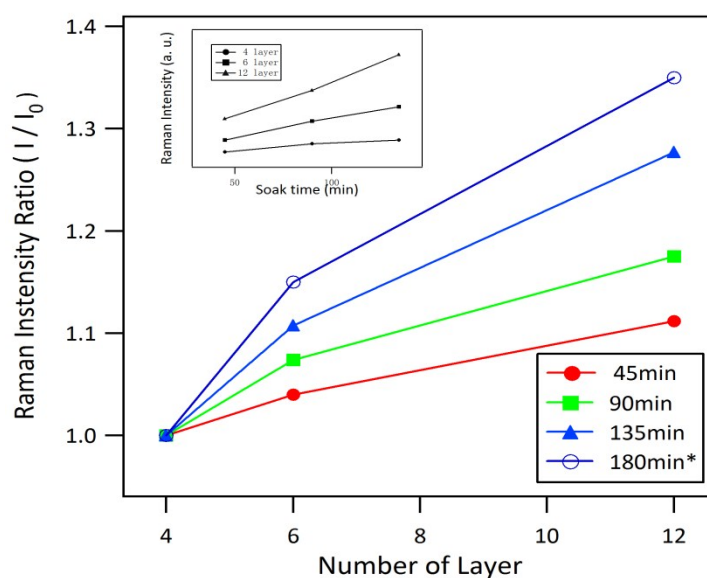


Figure S8. The Raman intensity ratio for different layers of horizontal assemblies measured after soaking in 4-MBA for different time. 45, 90, 135 mins data were taken at same positions of the same sample and were plotted as solid markers. *The 180min data is extracted from Figure 5d in the main text only for comparison. Thus it is for different sample and plotted with circle markers. Inset: time dependent Raman intensity of different layers.

In Figure S8, we show Raman intensity ratio vs. layers after soaking in 4-MBA ethanol solution for different period of time. As soaking time gets longer, The ratio of Raman signal from higher layer number to that from lowest layer number get stronger. This steady increase of Raman signal from high layer number vs. soaking time give a clear evidence that these increase of Raman signal is due to increase of 4-MBA molecules inside our superstructures. Combining this finding with steady increase of Raman signal with layer numbers, we can conclude we indeed observed SERS signal from as deep as 12 layers of NCs and prove SERS could propagate well inside our Au@Ag core-shell superstructures. But on the same time, the time dependent measurement also tell us number of 4-MBA molecules inside Au@Ag superstructures is far from forming monolayer coverage of NCs in the deeper layers. Indeed, forming a SAM on monolayer of NCs would take 3 hours, which is also the longest soaking time our current superstructure can endure without noticeable structure degradation. At this condition, diffusion of 4-MBA into the superstructure and thus efficient coverage NCs' surface for SERS application is still challenging. Further optimization of assembly method and SERS molecule loading are needed.

References

1. Y. Okuno, K. Nishioka, A. Kiya, N. Nakashima, A. Ishibashi and Y. Niidome, *Nanoscale*, 2010, 2, 1489-1493.
2. R. B. Jiang, H. J. Chen, L. Shao, Q. Li and J. F. Wang, *Adv. Mater.*, 2012, 24, OP200-OP207.
3. S. Liu, R. Jiang, P. You, X. Zhu, J. Wang and F. Yan, *Energy Environ. Sci.*, 2016, 9, 898-905.
4. W. Ni, X. Kou, Z. Yang and J. F. Wang, *ACS Nano*, 2008, 2, 677-686.
5. Y. Xie, S. Guo, C. Guo, M. He, D. Chen, Y. Ji, Z. Chen, X. Wu, Q. Liu and S. Xie, *Langmuir*, 2013, 29, 6232-6241.
6. P. B. Johnson and R. W. Christy, *Phys. Rev. B*, 1972, 6, 4370-4379.
7. E. D. Palik, *Handbook of optical constants of solids*, Academic press, 1998.